Resonant electron-phonon coupling: Magnetopolarons in InP

V. López and F. Comas
Department of Theoretical Physics, Havana University, Vedado 10400, Havana, Cuba

C. Trallero-Giner,* T. Ruf, and M. Cardona
Max-Planck-Institut für Festkörperforschung, Heisenbergstrasse 1, D-70569 Stuttgart, Federal Republic of Germany

(Received 28 May 1996)

We present a theoretical analysis of recent experimental data on resonant magnetopolarons in InP. These effects appear as strong anticrossings in Landau-level fan plots obtained from magneto-Raman profiles of the longitudinal-optic (LO)-phonon scattering intensity vs magnetic field. We calculate renormalized Landau levels using electron self-energies due to Fröhlich electron–LO-phonon interaction, and find an analytical expression for the self-energy of the magnetopolaron quasiparticle. A Green's-function treatment leads to close agreement with the experiment, even though we use relatively simple approximations for the self-energy. We find that the data can only be explained when couplings between adjacent Landau levels are taken into account. At this point our model supersedes previous theories, where resonant magnetopolarons have been approximated by two-level systems. [S0163-1829(96)04139-2]

I. INTRODUCTION

The present work is concerned with a theoretical investigation of recent experimental results on magnetopolaron resonances in InP which have been measured for a wide range of energies and magnetic fields by magneto-Raman spectroscopy.[1,2] In this technique, fan plots of resonance energies vs magnetic field are obtained from the enhancement of the LO-phonon Raman-scattering intensity which occurs when either incoming or scattered photons coincide with interband magneto-optical transitions between Landau levels. The analysis of fan plots yields information on basic properties of the electronic structure such as effective masses and g factors, the mixing of valence-band wave functions, or band nonparabolicity. Furthermore it allows one to investigate modifications of electronic states due to perturbations such as Coulomb interaction (exciton effects) and electron-phonon coupling (resonant and nonresonant polarons).

Magnetopolaron resonances have been investigated both theoretically and experimentally for a long time, particularly in bulk semiconductors.[3–9] In recent theoretical studies these effects have been calculated using modified Wigner-Brillouin perturbation theory.[10–12] In the usual (nonresonant) magnetopolaron effect, Landau levels are shifted to lower energies, and the slopes of fan lines change due to mass renormalization. Resonant anticrossings, however, appear when the energies of higher levels $|N\rangle$ (Landau indices $N=1,2,\ldots$) are comparable to that of the ($N=0$) Landau state plus the energy of an LO-phonon $\hbar\omega_{\mathrm{LO}}$, denoted in the following as $|N=0,1\mathrm{LO}\rangle$. Due to electron-phonon interaction, such states couple. In a simple picture of two interacting levels, one obtains an energy splitting which lifts the degeneracy at each crossing point. As a consequence of these magnetopolaron resonances each Landau level is split into two branches: a lower one which is pinned to the energy of the so-called polaron threshold, i.e., the energy of the $|N=0,1\mathrm{LO}\rangle$-state at high magnetic fields; and an upper one which approaches the same threshold at low magnetic fields.

Recent magneto-Raman experiments on the weakly polar semiconductor InP ($\alpha=0.11$, where α is the standard Fröhlich constant) described in Ref. 2 have revealed additional aspects of resonant magnetopolaron coupling which are beyond this simple picture. In that work, magnetopolaron resonances have been investigated over a wide range of magnetic fields up to 14 T. After subtraction of valence-band contributions and excitonic corrections which had been determined previously (see Refs. 1 and 13), fan plots of *electron* Landau states were obtained from which the energies and anticrossings of levels with indices up to $N=7$ could be analyzed. It was found that Landau levels $|N\rangle$ do not become pinned at the polaron threshold, where their intensity should rapidly decrease due to mixing with the $|N=0,1\mathrm{LO}\rangle$ state. On the contrary, they can be observed over a much wider range of energies and magnetic fields, and their slopes are significantly different than those expected from the pure pinning effect. The lower branch of the state $|N\rangle$ becomes the upper branch of $|N-1\rangle$ beyond the region of resonant coupling, and vice versa. The simple theoretical analysis in terms of two-level models cannot explain these observations. According to Ref. 2, this effect can be understood if a coupling between neighboring Landau states via their interaction with the polaron threshold state is taken into account.

The renormalization of Landau levels due to electron–LO-phonon interaction was calculated in Ref. 11 within second-order perturbation theory. As a function of the Landau-level index N, the total splitting at a magnetopolaron resonance for $\alpha\ll1$ was found to be[11]

$$\Delta E(N)=2\hbar\omega_{\mathrm{LO}}(\alpha/2N)^{2/3}. \quad (1)$$

This result is a generalization obtained by the application of improved Wigner-Brillouin perturbation theory described in Ref. 10 to all Landau levels at arbitrary magnetic fields. In the model of Ref. 2 the splittings given by Eq. (1) were phenomenologically introduced as off-diagonal coupling constants between the $|N\rangle$ and $|N=0,1\mathrm{LO}\rangle$ Landau states, and the experimental fan plots could be reproduced well.

In the present work we give a rigorous description of magnetopolaron resonances on the basis of a systematic Green's-function formalism which confirms the fundamental ideas discussed in Ref. 2. We find that the peculiarities of the fan plots just mentioned can be understood if the coupling of each Landau level with all the others is taken into account by means of a systematic consideration of electron–LO-phonon interaction via the Fröhlich Hamiltonian. This leads to a self-energy which renormalizes the Landau levels and includes the coupling of different states in a natural way. We obtain a rather good agreement with the experimental curves,[2] even within a relatively simple approximation for the self-energy which can be expressed by a compact mathematical expression. Similarly, the lifetime broadening, which is important especially for the higher Landau levels, is calculated vs magnetic field.

The paper is organized as follows: In Sec. II, we briefly outline the general theoretical background of the model and our calculations of the self-energy. In Sec. III, we give a discussion of the results and compare them with the experimental data. Some technical aspects of the theory are summarized in the Appendix.

II. GENERAL THEORY AND CALCULATIONS

The energy levels of an electron in a simple parabolic conduction band with the effective electron mass m^* and a magnetic field B, described by the Landau gauge $\vec{A}\equiv(0,Bx,0)$, are given by

$$E_N(k_3)=\hbar\omega_c(N+\tfrac{1}{2})+\frac{\hbar^2k_3^2}{2m^*}, \tag{2}$$

where $\omega_c=eB/m^*c$ is the cyclotron frequency, $N=0,1,2\ldots$ the Landau index, and $\vec{k}=(k_1,k_2,k_3)$ the crystal-momentum vector. The electron–LO-phonon interaction has not yet been taken into account. The wave functions are

$$\Psi=\frac{1}{\sqrt{L^2}}e^{ik_2y+ik_3z}\varphi_N(x-x_0), \tag{3}$$

where

$$\varphi_N(x-x_0)=\gamma^{-1/2}\exp\left[-\frac{1}{2}\left(\frac{x-x_0}{\gamma}\right)\right]\frac{H_N\left(\frac{x-x_0}{\gamma}\right)}{\sqrt{2^NN!\sqrt{\pi}}}, \tag{4}$$

and $\gamma=(\hbar c/Be)^{1/2}$ is the magnetic length, and L is the normalization length, $x_0=-\gamma^2k_2$ and $H_N(\xi)$ are the Hermite polynomials.[14] In Eq. (2) the spin interaction with the magnetic field is neglected. It can be easily added in all expressions obtained by introducing the appropriate g factor.[15]

The $T=0$-K one-particle Green's function for the electron (considering just the one-electron case) in the magnetic field is defined by[16]

$$G(k_3,x,x',E)=\hbar\sum_N\frac{\varphi_N(x-x_0)\varphi_N(x'-x_0')}{E-E_N(k_3)+i\delta}, \tag{5}$$

where $\delta\to+0$, the Fourier transform has been taken for the coordinates y and z, and E is the energy parameter. This Green's function is easily transformed into a representation in terms of Landau levels $G_0(k_3,N,N',E)$ by means of

$$G_0(k_3,N,N',E)=\int_{-\infty}^{\infty}\int_{-\infty}^{\infty}\varphi_N(x-x_0)\varphi_{N'}(x'-x_0')\times G(k_3,x,x',E)dx\,dx', \tag{6}$$

leading to

$$G_0(k_3,N,N',E)=\delta_{NN'}G_0(k_3,N,E), \tag{7}$$

where

$$G_0(k_3,N,E)=\frac{\hbar}{E-E_N(k_3)+i\delta}. \tag{8}$$

On the other hand, the Fröhlich-interaction Hamiltonian in a completely second-quantized description is given by[17]

$$\hat{H}_{e\text{-}ph}=\sum_{\vec{k},\vec{q},N,N'}C_{\vec{q}}L_{NN'}(q_1)\hat{B}_{\vec{q}}\hat{a}^+_{\vec{k}+\vec{q},N}\hat{a}_{\vec{k},N'}, \tag{9}$$

where

$$C_{\vec{q}}=-i\left(\frac{2\pi\hbar\omega_{\vec{q}}e^2}{q^2L^3}(\varepsilon_\infty^{-1}-\varepsilon_0^{-1})\right)^{1/2}, \tag{10}$$

ε_0 (ε_∞) is the static (high frequency) dielectric constant; $\hbar\omega_{\vec{q}}$ the LO-phonon energy, $\vec{q}$ the phonon wave vector; $\hat{B}_{\vec{q}}=\hat{b}_{\vec{q}}+\hat{b}^+_{-\vec{q}}$, with the LO-phonon annihilation (creation) operators $\hat{b}_{\vec{q}}$ ($\hat{b}^+_{\vec{q}}$), $\hat{a}_{\vec{k}N}$ ($\hat{a}^+_{\vec{k}N}$), the electron annihilation (creation) operator with energy $E_N(k_3)$; and

$$L_{NN'}(q_1,k_2,k_2')=\int_{-\infty}^{\infty}\varphi_N[x-x_0(k_2)]\varphi_{N'}[x-x_0(k_2')]\times e^{iq_1x}dx. \tag{11}$$

It is well known that the phonon Green's function is defined by[18]

$$D_0(\vec{q},\omega)=\frac{2\omega_{\vec{q}}}{\omega^2-\omega_{\vec{q}}^2+i\delta};\quad \delta\to+0. \tag{12}$$

The Dyson equation for the motion of an electron being simultaneously subjected to a magnetic field $\vec{B}$ and to the electron–LO-phonon interaction is diagrammatically presented in Fig. 1(a), where $G_0(k_3,N,E)$ represents the unperturbed Green's function and $M(k_3,N,N_2,E)$ the irreducible self-energy. As discussed in Refs. 3 and 4, the self-energy can be approximated to lowest order in the coupling constant α (due to electron–LO-phonon interaction) by the diagram shown in Fig. 1(b). In this approximation the Dyson equation reduces to

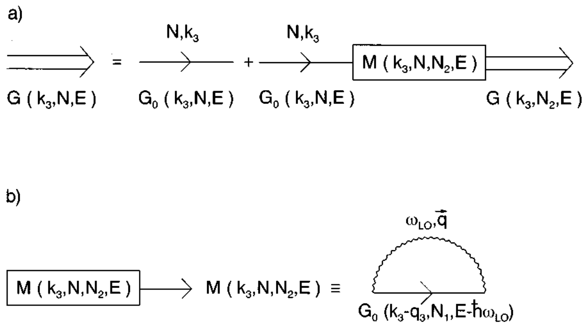

FIG. 1. (a) Dyson equation for the magnetopolaron process. Solid lines represent the Green's function $G_0(k_3,N,E)$ of an electron in an external magnetic field. (b) The irreducible self-energy part $M(k_3,N,N_2,E)$ in the lowest order of the electron–LO-phonon coupling constant. The wavy line symbolizes the unperturbed phonon Green's function.

$$
\begin{aligned}
G(k_3,N,E) \\
&= G_0(k_3,N,E)\Bigg[1+\sum_{N_1,N_2,\vec{q}} |C_{\vec{q}}|^2 L_{NN_1}(q_1,k_2-q_2,k_2) \\
&\quad \times L^*_{N_1N_2}(q_1,k_2,k_2-q_2) \\
&\quad \times G_0(k_3-q_3,N_1,E-\hbar\omega_{\vec{q}})G(k_3,N_2,E)\Bigg]. \qquad (13)
\end{aligned}
$$

In the general case, no self-energy part can be separated from the rest of the diagram. For the matrix element L_{NN_1} the integral over the spatial coordinate can be performed exactly, thus leading to[19]

$$
\begin{aligned}
L_{NN_1} &= 2^{|N_1-N|/2}\min\left[\left(\frac{N_1!}{N!}\right)^{1/2};\left(\frac{N!}{N_1!}\right)^{1/2}\right] \\
&\quad \times e^{-\frac{q_\perp}{2}} L^{|N_1-N|}_{\min[N;N_1]}\left(\frac{q_\perp^2}{2}\right) \\
&\quad \times \left(\operatorname{sgn}[N_1-N]\frac{q_2}{2}-i\frac{q_1}{2}\right)^{|N_1-N|}, \qquad (14)
\end{aligned}
$$

where $\operatorname{sgn}[z]=1\ (-1)$ if $z>0\ (z<0)$, $q_\perp^2=q_1^2+q_2^2$, and $L_n^m(z)$ are the generalized Laguerre polynomials. Considering dispersionless LO phonons ($\omega_{\vec{q}}\rightarrow\omega_{\rm LO}$) and the Dyson equation just for $k_3=0$, we are led to

$$
\begin{aligned}
G(0,N,E) &= G_0(0,N,E) \\
&\quad \times\left[1+\sum_{N_2} M(0,N,N_2,E)G(0,N_2,E)\right]. \qquad (15)
\end{aligned}
$$

Transforming the summation over $\vec{q}$ into integrals (in the standard way) we finally obtain the following self-energy (see some details in the Appendix):

$$
\begin{aligned}
M(0,N,N_2,E) &= M(N,E)\,\delta_{NN_2} \\
&= \frac{e^2}{\gamma}(\varepsilon_\infty^{-1}-\varepsilon_0^{-1})\left(-\frac{\omega_{\rm LO}}{\omega_c}\right)\sum_{N_1}\min\left[\frac{N_1!}{N!};\frac{N!}{N_1!}\right]\frac{e^{\frac{Q}{2}}(n_{\min}+m)!}{2\sqrt{Q}\,2^{2n_{\min}}n_{\min}!}\sum_{k=0}^{n_{\min}}\binom{2(n_{\min}-k)}{n_{\min}-k}\frac{(2k)!}{k!}\frac{1}{(m+k)!} \\
&\quad \times\sum_{j=0}^{2k}(-1)^j\binom{2(m+k)}{2k-j}\frac{1}{j!}\left\{\left(\frac{Q}{2}\right)^{m+j}\left[i\Gamma(m+j+1)\Gamma\left(-[m+j];\frac{Q}{2}\right)\right.\right. \\
&\quad \left.\left.-\Gamma(m+j+\tfrac{1}{2})\Gamma\left(\frac{1}{2}-[m+j];\frac{Q}{2}\right)\right]\right\}\delta_{NN_2}, \qquad (16)
\end{aligned}
$$

with

$$n_{\min}\equiv\min[N_1;N],$$

$$m\equiv|N_1-N|,$$

$$\binom{p}{q}\equiv\frac{p!}{q!(p-q)!},$$

$$Q\equiv\frac{2\omega_{\rm LO}}{\omega_c}\left(\frac{E}{\hbar\omega_{\rm LO}}-\frac{\omega_c}{\omega_{\rm LO}}[N_1+\tfrac{1}{2}]-1+i\frac{\delta}{\hbar\omega_{\rm LO}}\right).$$

It is worth mentioning that a selection rule is obtained, forbidding transitions between initial and final states with different N which simplifies the expressions. The self-energy of Eq. (16) involves a summation over all Landau levels in order to renormalize the Nth state. In this way our treatment introduces directly the above mentioned couplings between different Landau levels.

In order to determine the renormalized energy spectrum for conduction electrons as well as their life-time broadening we need to solve the real and imaginary parts of the transcendental equation (for $k_3=0$)

$$E=\hbar\omega_c(N+\tfrac{1}{2})+M(N,E), \qquad (17)$$

which is done numerically by applying an iterative method. The equations involved in this procedure are

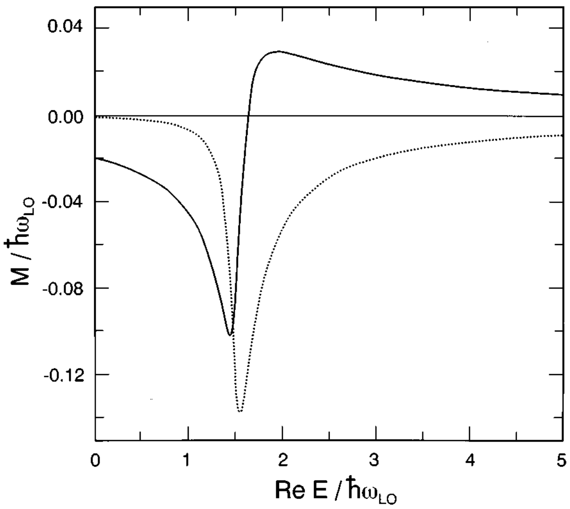

FIG. 2. Resonant part of the self-energy $M(0,N,E)$ for electrons in InP with $N=1$, $N_1=0$, and $\omega_c=\omega_{\rm LO}$, and a level width of $\delta=4.3$ meV. The solid line represents the real part of the self-energy, and the dotted line the corresponding imaginary part. Energies are given in units of $\hbar\omega_{\rm LO}$.

$$\mathrm{Re}E=\hbar\omega_c\left(N+\frac{1}{2}\right)+\mathrm{Re}M(N,\mathrm{Re}E,\mathrm{Im}E)$$

$$\mathrm{Im}E=\mathrm{Im}M(N,\mathrm{Re}E,\mathrm{Im}E). \tag{18}$$

III. RESULTS AND DISCUSSION

In Fig. 2 we show the real (solid line) and imaginary (dotted line) parts of $M(N,E)$ as given by Eq. (16) vs ReE. The following parameters for bulk InP were used: $m^*=0.077m_0$,[20] where m_0 is the free-electron mass; $\hbar\omega_{\rm LO}=43$ meV;[21] $\varepsilon_0=12.6$; $\varepsilon_\infty=9.6$;[20] and the broadening parameter $\delta=4.3$ meV. The curves were calculated for $N=1$ and $N_1=0$ and, in the resonance region, we set $\omega_c=\omega_{\rm LO}$. As can be seen from Fig. 2, resonance occurs near $\mathrm{Re}E\simeq1.5\hbar\omega_{\rm LO}$, in agreement with the expression $E/\hbar\omega_{\rm LO}=(\omega_c/\omega_{\rm LO})(N_1+\frac{1}{2})+1$, i.e., when for a given magnetic field two Landau levels (not necessarily consecutive ones) are separated by the LO-phonon energy $\hbar\omega_{\rm LO}$. The imaginary part of $M(N,E)$ in Fig. 2 is related to the electron lifetime broadening. An example of the enhancement of the level width near resonance is shown in Fig. 3, where the lifetime broadening (ImE) vs $\omega_c/\omega_{\rm LO}$ is given for the third perturbed Landau level ($N=2$, $N_1=0$).

The fundamental result of this paper is shown in Fig. 4. Plotting the renormalized Landau levels (ReE) vs magnetic field (solid lines), we obtain fanlike spectra with characteristic anticrossings as found experimentally for the lowest polaron threshold in Ref. 2. The dashed lines describe the unperturbed system. Note that renormalization leads to a different arrangement of Landau levels which exhibits a staircaselike structure reflecting coupled two-level systems. Near resonance, the levels are no longer pinned at the polaron threshold, but rather pick up the character of adjacent levels, following their course after having moved through a subsequent resonance.

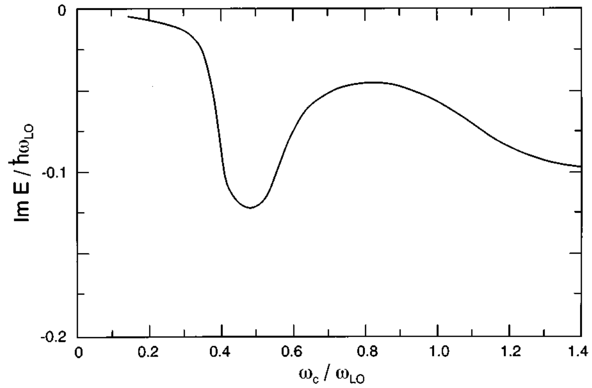

FIG. 3. Imaginary part of the magnetopolaron energy vs magnetic field in InP for the third perturbed Landau level ($N=2$, $N_1=0$). This quantity is related to the lifetime broadening. Energies are given in units of $\hbar\omega_{\rm LO}$, and B is expressed by the relative cyclotron frequency $\omega_c/\omega_{\rm LO}$.

Figure 5 shows a comparison of our theory with experimental data from Ref. 2. The solid lines represent the renormalized Landau levels calculated according to Eq. (18). The data points (open circles), obtained from interband magneto-Raman resonances [$\overline{z(\sigma^-,\sigma^+)}z$ geometry] after the subtraction of valence band and exciton contributions and the energy of one LO phonon to account for their outgoing character,[1,2,13] almost coincide with these curves. Hence the Green's-function calculation leads, even within a relatively simple approximation for the self-energy, to a very good description of the experimental results. Such close agreement

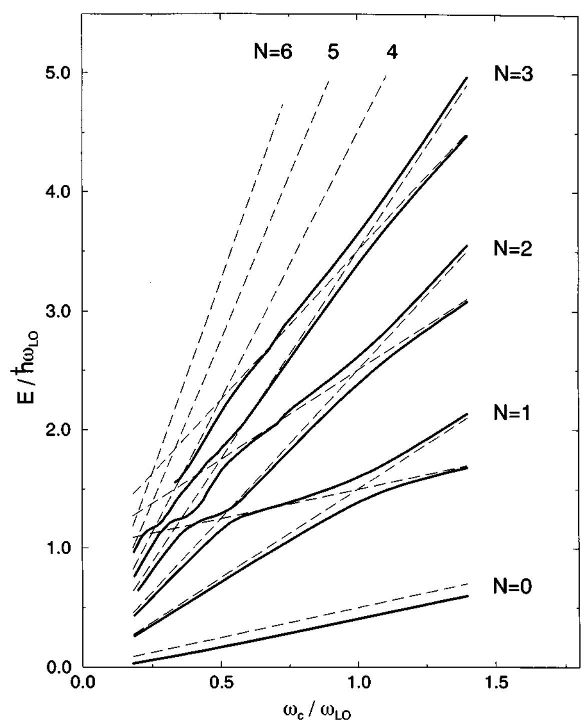

FIG. 4. Real part of the magnetopolaron energies vs magnetic field. Energies are given in units of $\hbar\omega_{\rm LO}$, and B is expressed by the relative cyclotron frequency $\omega_c/\omega_{\rm LO}$. The dashed lines represent unperturbed electron Landau levels with indices N.

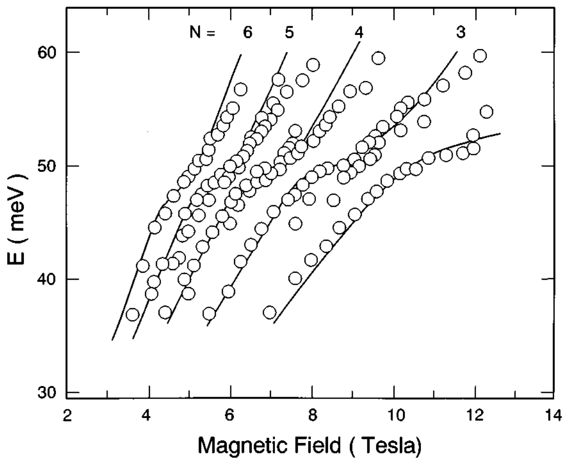

FIG. 5. Electron energy levels vs magnetic field for InP. The open circles correspond to experimental data (Ref. 2) from magneto-Raman scattering for the $\overline{z(\sigma^-,\sigma^+)z}$ configuration, solid lines represent theoretical calculations according to Eq. (17).

with experiment can be achieved only when couplings with other Landau levels are taken into account in the renormalization of the states. These results also confirm the theoretically predicted dependence of the magnitude of the polaron splittings on the Landau-level index given by Eq. (1).

Figure 6 illustrates the consequences of these differences between the simple description of magnetopolaron resonances in a two-level picture [Fig. 6(a)], and changes due to the more complete treatment given here [Fig. 6(b)] for magneto-optical *interband* transitions, which are observed experimentally in magneto-Raman profiles. To be specific, we consider the magnetopolaron resonance between the threshold and the $N=5$ Landau state. We use effective masses of $m_e^*=0.077m_0$ and $m_{\text{lh}}^*=0.12m_0$ for electrons and holes, resulting in slopes $\hbar e/m^*$ of about 1.5 and 1.0 meV/T for the fan lines, respectively, and $\hbar\omega_{\text{LO}}=43$ meV.[20] For simplicity, g factors have been neglected. Interband transitions, involving electron and hole states, are denoted by E_n^m in the following, where the lower (upper) number gives the hole (electron) Landau index, respectively. The pure *electronic* levels for $N=5$ and the (lowest) polaron threshold state are denoted by E^5 and $E^{0,\text{LO}}$, respectively. In *interband* transitions the polaron threshold is observed via the renormalization of the electron part of the E_n^m fan lines. The relevant asymptotes are thus $E_n^{0,\text{LO}}$. The solid lines in Fig. 6(a) are resonances of E_5^5 expected in a two-level model if one assumes that mixing with the threshold $E_5^{0,\text{LO}}$, which is approached asymptotically by the renormalized states, reduces its wave function such that it can only be observed within 1 T of the crossing point. The unrenormalized states are indicated by dashed lines. Let us now consider the coupling of E_5^5 with neighboring transitions shown in Fig. 6(b). Approaching the threshold from lower (higher) energies, it first bends over toward $E_5^{0,\text{LO}}$. However, before reaching the transition with the next lower (higher) index, its curvature changes again, and it follows along fan lines for which the *electron* Landau index has been lowered (raised) by one unit, i.e., E_5^4 (E_5^6). The hole index does not change at all. This behavior is indicated by the solid lines in Fig. 6(b), where we have again assumed that the resonances can be experimentally observed only within 1 T away from the anticrossing point. In contrast to Fig. 6(a), the renormalized fan lines approach significantly different asymptotes away from the resonance region. This case corresponds to our experimental observations.[1,2] Subtracting the hole Landau levels, we obtain results similar to those of Fig. 5. Note that a precise measurement of the slopes of renormalized interband transition fan lines in the quasiclassical limit (large N, small B) (Ref. 22) should allow one to determine not only the reduced effective mass but also the electron and hole mass separately.

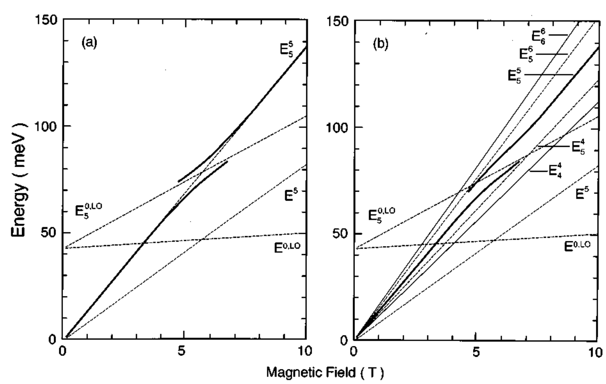

FIG. 6. Renormalization of magneto-optical *interband* transitions E_n^m between Landau levels due to resonant magnetopolarons presented schematically for the $N=5$ Landau level (solid lines). (a) Two-level system: fan lines of E_5^5 are pinned at the polaron threshold $E_5^{0,\text{LO}}$. (b) Coupling between different Landau levels and the resulting wave-function mixing significantly changes the course of fan lines across resonances. Dashed lines indicate unrenormalized transitions. E^5 and $E^{0,\text{LO}}$ denote *electron* parts of the $N=5$ Landau level and the lowest polaron threshold, respectively. See text for details.

IV. CONCLUSIONS

We have calculated magnetopolaron resonances in InP by a Green's-function method. Experimental fan plots obtained from magneto-Raman profiles can be explained only when coupling between more than two Landau levels is taken into account. A simple two-level model is not sufficient to describe the behavior of the fan lines away from resonance, where they are no longer pinned but take over the character of neighboring transitions. The dependence of the magnitude of resonant magnetopolaron splittings on the Landau level index is experimentally confirmed.

ACKNOWLEDGMENTS

Technical support by H. Hirt and M. Siemers is gratefully acknowledged. Thanks are due to A. Sirenko for a critical reading of the manuscript.

APPENDIX

In order to obtain Eq. (16), the following integrations were performed. From Eq. (13) the self-energy part can be written

$$M(0,N,N_2,E)=\sum_{N_1,\vec{q}}|C_{\vec{q}}|^2 L_{NN_1}(q_1,k_2-q_2,k_2) \times L^*_{N_1N_2}(q_1,k_2,k_2-q_2) \times G_0(k_3-q_3,N_1,E-\hbar\omega_{\vec{q}}). \quad \text{(A1)}$$

The summation over $\vec{q}$ in Eq. (A1) must be transformed into an integral in polar coodinates. Applying Eq. (14), with the substitution $\gamma q_i \rightarrow q_i$ and measuring energies in units of $\hbar\omega_{\mathrm{LO}}$ in order to obtain dimensionless quantities under the integral, we are led to

$$M(0,N,N_2,E)=\frac{e^2}{2\pi^2\gamma}(\varepsilon_\infty^{-1}-\varepsilon_0^{-1})\left(-\frac{\omega_{\mathrm{LO}}}{\omega_c}\right) \times \sum_{N_1}\int_0^\infty q_\perp dq_\perp \int_{-\infty}^{\infty}\frac{dq_3}{(q_3^2+q_\perp^2)(q_3^2-Q)} \times \int_0^{2\pi} d\theta\, L_{NN_1}L^*_{N_1N_2}. \quad \text{(A2)}$$

The integral over θ is

$$\int_0^{2\pi} d\theta\left(\mathrm{sgn}[N-N_1]\frac{q_\perp \sin\theta}{2}-i\frac{q_\perp\cos\theta}{2}\right)^{|N_1-N|} \times\left(\mathrm{sgn}[N_2-N_1]\frac{q_\perp\sin\theta}{2}+i\frac{q_\perp\cos\theta}{2}\right)^{|N_2-N_1|} =2\pi\left(\frac{q_\perp}{2}\right)^{2|N_1-N|}\delta_{N_1N_2}. \quad \text{(A3)}$$

Integrating over q_3, Eq. (A3) reduces to

$$M(0,N,E)=\frac{e^2}{\gamma}(\varepsilon_\infty^{-1}-\varepsilon_0^{-1})\left(-\frac{\omega_{\mathrm{LO}}}{\omega_c}\right) \times\sum_{N_1} 2^{-|N_1-N|}\min\left[\frac{N_1!}{N!};\frac{N!}{N_1!}\right] \times\int_0^\infty \frac{du\; e^{-(1/2)u}u^{|N_1-N|}}{2(u+Q)}\left(\frac{i}{\sqrt{Q}}-\frac{1}{\sqrt{u}}\right) \times\left[L^{|N_1-N|}_{\min[N;N_1]}\left(\frac{u}{2}\right)\right]^2. \quad \text{(A4)}$$

Equation (16) can be derived using the series expansion of generalized Laguerre polynomials[23]

$$\left[L_n^m\left(\frac{u}{2}\right)\right]^2=\frac{(n+m)!}{2^{2n}n!}\sum_{k=0}^{n}\binom{2(n-k)}{n-k}\frac{(2k)!}{k!}\frac{1}{(m+k)!} \times\sum_{j=0}^{2k}\frac{(-1)^j}{j!}\binom{2(m+k)}{2k-j}x^j, \quad \text{(A5)}$$

and expressing Eq. (A4) in terms of integrals of the form[23]

$$\int_0^\infty dx\,\frac{e^{-\mu x}x^{\nu-1}}{x+\beta}=\beta^{\nu-1}e^{\beta\mu}\Gamma(\nu)\Gamma(1-\nu;\beta\mu), \quad \text{(A6)}$$

where $|\arg\beta|<\pi$, $\mathrm{Re}\mu>0$, and $\Gamma(\xi)$ $[\Gamma(\xi;\eta)]$ are the complete (incomplete) gamma functions.

*On leave from Department of Theoretical Physics, Havana University, 10400 Havana, Cuba.

[1] T. Ruf, R. T. Phillips, A. Cantarero, G. Ambrazevičius, M. Cardona, J. Schmitz, and U. Rössler, Phys. Rev. B **39**, 1378 (1989).
[2] F. Iikawa, T. Ruf, and M. Cardona, in *High Magnetic Fields in the Physics of Semiconductors*, edited by D. Heimann (World Scientific, Singapore, 1995), p. 690.
[3] V. L. Gurevich and Yu. A. Firzov, Zh. Éksp. Teor. Fiz. **40**, 198 (1961) [Sov. Phys. JETP **13**, 137 (1961)].
[4] L. I. Korovin and S. T. Pavlov, Zh. Éksp. Teor. Fiz. **53**, 1708 (1967) [Sov. Phys. JETP **26**, 979 (1968)].
[5] M. Nakayama, J. Phys. Soc. Jpn. **27**, 636 (1969).
[6] D. M. Larsen, Phys. Rev. **135**, A419 (1964); **180**, 919 (1969).
[7] D. M. Larsen and E. J. Johnson, J. Phys. Soc. Jpn. Suppl. **21**, 443 (1966).
[8] D. M. Dickey, E. J. Johnson, and D. M. Larsen, Phys. Rev. Lett. **18**, 599 (1967).
[9] D. M. Larsen, in *Polarons in Ionic Crystals and Polar Semiconductors*, edited by J. T. Devreese (North-Holland, Amsterdam, 1972), p. 237, and references therein.
[10] G. Lindemann, R. Lassnig, W. Seidenbusch, and E. Gornik, Phys. Rev. B **28**, 4693 (1983).
[11] F. M. Peeters and J. T. Devreese, Phys. Rev. B **31**, 3689 (1985).
[12] P. Pfeffer and W. Zawadzki, Solid State Commun. **57**, 847 (1986).
[13] F. Iikawa, T. Ruf, and M. Cardona, Phys. Rev. B **43**, 4849 (1991).
[14] *Handbook of Mathematical Functions*, edited by M. Abramowitz and I. Stegun (Dover, New York, 1972).
[15] C. Trallero-Giner, T. Ruf, and M. Cardona, Phys. Rev. B **41**, 3028 (1990).
[16] As a general reference to Green's function theory, see, for example, the book by G. D. Mahan, *Many-Particle Physics* (Plenum, New York, 1990).
[17] H. Fröhlich, H. Pelzer, and S. Zienau, Philos. Mag. **41**, 221 (1950).
[18] A. S. Davydov, *Solid State Theory* (Mir, Moscow, 1981).
[19] A. Erdelyi *et al.*, *Higher Trascendental Functions* (McGraw-Hill, New York, 1953), Vol. 1.
[20] *Semiconductors. Intrinsic Properties of Group IV Elements and III-V, II-VI, and I-VIII Compounds*, edited by O. Madelung, H. Schultz, and H. Weiss, Landolt-Bornstein, New Series, Vol. III, Vol. 22, Pt. a (Springer-Verlag, Berlin, 1982).
[21] A. Mooradian and G. B. Wright, Solid State Commun. **4**, 431 (1966).
[22] S. I. Gubarev, T. Ruf, M. Cardona, and K. Ploog, Phys. Rev. B **48**, 1647 (1993).
[23] I. S. Gradshteyn and I. M. Ryzhyk, *Table of Integrals, Series and Products* (Academic, London, 1970).